Reduced expression of *MECP2* affects cell commitment and maintenance in neurons by triggering senescence: new perspective for Rett syndrome

Tiziana Squillaro[a,b], Nicola Alessio[c,d], Marilena Cipollaro[a], Mariarosa Anna Beatrice Melone[e], Giuseppe Hayek[f], Alessandra Renieri[g], Antonio Giordano[b,c,h], and Umberto Galderisi[a,b,c]

[a]Department of Experimental Medicine, Biotechnology and Molecular Biology Section, Second University of Naples, 80138 Naples, Italy; [b]Human Health Foundation, 06049 Spoleto, Italy; [c]Sbarro Institute for Cancer Research and Molecular Medicine, Center for Biotechnology, Temple University, Philadelphia, PA 19122; [d]Department of Biomedical Sciences, University of Sassari, 07100 Sassari, Italy; [e]Dipartimento Medico-Chirurgico di Internistica Clinica e Sperimentale "F. Magrassi e A. Lanzara," 80100 Naples, Italy; [f]Childhood Neuropsychiatry, Azienda Ospedaliera Senese, 53100 Siena, Italy; [g]Medical Genetics and [h]Human Pathology and Oncology Department, University of Siena, 53100 Siena, Italy

ABSTRACT **MECP2 protein binds preferentially to methylated CpGs and regulates gene expression by causing changes in chromatin structure. The mechanism by which impaired MECP2 activity can induce pathological abnormalities in the nervous system of patients with Rett syndrome (RTT) is not clearly understood. To gain further insight into the role of MECP2 in human neurogenesis, we compared the neural differentiation process in mesenchymal stem cells (MSCs) obtained from a RTT patient and from healthy donors. We further analyzed neural differentiation in a human neuroblastoma cell line carrying a partially silenced *MECP2* gene. Senescence and reduced expression of neural markers were observed in proliferating and differentiating MSCs from the RTT patient, which suggests that impaired activity of MECP2 protein may impair neural differentiation, as observed in RTT patients. Next, we used an inducible expression system to silence *MECP2* in neuroblastoma cells before and after the induction of neural differentiation via retinoic acid treatment. This approach was used to test whether MECP2 inactivation affected the cell fate of neural progenitors and/or neuronal differentiation and maintenance. Overall, our data suggest that neural cell fate and neuronal maintenance may be perturbed by senescence triggered by impaired MECP2 activity either before or after neural differentiation.**

Monitoring Editor
Carl-Henrik Heldin
Ludwig Institute for Cancer Research

Received: Sep 15, 2011
Revised: Feb 7, 2012
Accepted: Feb 13, 2012

INTRODUCTION

Rett syndrome (RTT) is one of the most common genetic causes of mental retardation in young females. In 1999, mutations in the *MECP2* gene were identified in up to 90% of RTT patients (Weaving *et al.*, 2005).

The MECP2 protein binds to methylated CpG dinucleotides and mediates gene silencing by causing changes in chromatin structure through interactions with corepressors such as histone deacetylases (Jones *et al.*, 1998). MECP2 may also interact with other chromatin-modifying enzymes, such as histone methyltransferases, BRM, SWI/SNF, and ATRX (Fuks *et al.*, 2003; Harikrishnan *et al.*, 2005; Giorgio *et al.*, 2007). Of interest, MECP2 also interacts with the DNA methyltransferase DNMT1, and thus it could be involved in the regulation of DNA methylation (Kimura and Shiota, 2003). Recent studies showed that the function of MECP2 extends beyond gene silencing, which demonstrates that MECP2 may act as a transcriptional modulator rather than a transcriptional repressor (Yasui *et al.*, 2007).

This article was published online ahead of print in MBoC in Press (http://www.molbiolcell.org/cgi/doi/10.1091/mbc.E11-09-0784) on February 22, 2012.

T.S. and N.A. performed research; M.C. performed research and analyzed data; A.R., M.A.B.M., and A.G. contributed vital new reagents and analytical tools and analyzed data; U.G. performed research, analyzed data, and wrote the article.

Address correspondence to: Umberto Galderisi (umberto.galderisi@unina2.It).

Abbreviations used: BrdU, bromodeoxyuridine; MSCs, mesenchymal stem cells; RTT, Rett.

The MECP2 protein is found in most tissues and cell types, but the highest expression levels of this protein are detected in the brain (Tudor *et al.*, 2002; Luikenhuis *et al.*, 2004). MECP2 is present in different regions of developing rat brains beginning at late embryonic stages. The protein levels of MECP2 correlate with neural maturation and synapse formation because MECP2 expression increases as cells acquire a mature neural phenotype (Jung *et al.*, 2003; Mullaney *et al.*, 2004). Several *MECP2*-knockout models have been generated (Chen *et al.*, 2001; Guy *et al.*, 2001; Shahbazian *et al.*, 2002). One of these models demonstrated that deletion of this gene in postmitotic neurons resulted in a RTT-like phenotype, which suggested that MECP2 might be important for neural maturation and maintenance rather than early cell fate decisions or neuronal development (Chen *et al.*, 2001; Tudor *et al.*, 2002; Luikenhuis *et al.*, 2004). Despite the existence of a large amount of data on the role of MECP2 as the causative gene in RTT syndrome, several questions remain unanswered. In fact, it is difficult to reconcile the relatively restricted pathology of RTT with the widespread expression pattern of *MECP2* and its promiscuous binding to chromosomes.

However, the general role of *MECP2* as a transcriptional regulator cannot be excluded from analysis because assessment of the phenotype of patients with RTT and analysis of *MECP2*-deficient mice has been performed primarily with respect to neuronal function. Furthermore, more subtle deficiencies outside and inside the CNS might have been overlooked (Shahbazian *et al.*, 2002).

Therefore, in the present study, we investigated the biology of bone marrow–derived mesenchymal stem cells (MSCs) in RTT patients to determine whether mutations in the *MECP2* gene can result in an alteration of stem cell biology (Squillaro *et al.*, 2008a, 2008b, 2008c).

We hypothesized that the study of MSCs in RTT patients would be of interest for the following reasons: 1) MSCs play a key role in the homeostasis of many organs and tissues, and 2) in neurodevelopmental disorders such as RTT, neural stem cells should be analyzed to detect possible alterations in neuronal/glial commitment and differentiation. Clearly, neural stem cells cannot be obtained from RTT patients. Therefore MSCs represent a valid alternative in which to study neurogenesis because they can differentiate into neurons and glia. In our previous studies, we demonstrated that MSCs from RTT patients display early signs of senescence (Squillaro *et al.*, 2008a, 2008b, 2008c).

Data obtained using MSCs from RTT patients correlated with those obtained using control MSCs in which *MECP2* was silenced. Partial silencing of *MECP2* in human MSCs induced a significant reduction of S-phase cells and an increase in G_1 cells. These changes were accompanied by reduction in apoptosis, triggering of senescence, decrease in telomerase activity, and down-regulation of the genes involved in maintaining stem cell properties (Squillaro *et al.*, 2010).

In the present study, we compared the neural differentiation process in MSCs obtained from a RTT patient and from healthy donors. We also analyzed neural differentiation in a human neuroblastoma cell line carrying a partially silenced *MECP2* gene. Using both models, we demonstrate that the senescence phenomena may impair neural maturation processes.

RESULTS

MECP2 mutation affects MSC biology

An enrolled RTT patient presented the clinical manifestations of classic Rett syndrome. She carried a de novo mutation (R270X) in the *MECP2* gene (Supplemental File 1). We obtained MSCs from this patient and from two healthy controls as described in *Materials and Methods*. Following an initial expansion for 7–10 d, the MSCs reached confluence and were grown for an additional 10 d. At the end of this period, the MSCs were collected for biological assays or were further cultivated for neural differentiation.

Proliferating MSCs from the RTT patient and controls were determined by fluorescence-activated cell sorting (FACS) analysis. In several experiments, we observed a significant reduction ($p < 0.05$) in S-phase cells and an increase in G_1/G_0 ($p < 0.05$) and G_2/M cells in the RTT sample compared with controls (Figure 1A).

The MSCs were obtained from a RTT patient who had a mosaic expression of mutated and wild-type MECP2 due to X chromosome inactivation. Because the patient had a mutation that produced C-terminal–truncated proteins, we used a C-terminal–specific anti-MeCP2 antibody, combined with biological assays, to specifically analyze the MECP2-mutated cells (MECP2 negative by immunofluorescence). The analysis of somatic mosaicism in MSCs from the RTT patient evidenced 61.5% (±5.0%) of MECP2-positive cells (wild-type cells) and 38.5% (±5.9%) of MECP2-negative cells (mutated cells).

The bromodeoxyuridine (BrdU) assay showed that reduction in proliferation, as detected with FACS analysis, affected only cells with inactivated MECP2, as evidenced by the double-staining assay (Figure 1B).

The annexin assays showed a significant reduction ($p < 0.05$) of apoptotic cells in MECP2 cultures obtained from the RTT sample as compared with those from controls (Figure 1C). Moreover, signs of senescence were detected more in cells from the RTT patient than in those from healthy donors, as found by the in situ acid β-galactosidase assay (Figure 1D). In addition, in this case, the impairment of cell function occurred in cells with the mutated form of MECP2 and was statistically significant ($p < 0.05$).

Senescent cells show several changes in gene expression, including changes in known cell-cycle inhibitors or activators. Two cell-cycle inhibitors that are often expressed by senescent cells are the cyclin-dependent kinase inhibitors (CDKIs) $p21^{Cip1}$ and $p16^{INK4a}$ (Campisi and d'Adda di Fagagna, 2007). These CDKIs are components of tumor-suppressor pathways that are governed by the p53 and retinoblastoma family proteins, respectively (Kapic *et al.*, 2006; Campisi and d'Adda di Fagagna, 2007; Helmbold *et al.*, 2009).

In proliferating cells from the RTT patient, we detected a significant up-regulation ($p < 0.05$) of the p53 protein level as compared with the control sample (Figure 1E). On the contrary, however, we did not find significant modifications of $p21^{Cip1}$, pRb, and $p16^{INK4a}$ protein expression (Figure 1E). Note that Western blots were carried out on the whole population of MSCs from the RTT patient containing mutated and wild-type MECP2 cells; hence, subtle changes in gene expression may might been overlooked.

Overall, these data confirm our previous results obtained in patients showing the clinical manifestations of classic and "fruste" Rett syndrome (Squillaro *et al.*, 2008a, 2008b, 2008c).

In vitro neural differentiation of MSCs from patient with classic RTT syndrome

A complete study of neural cell commitment and differentiation should be carried out with neural stem cells. Obviously, it is not possible to obtain neural stem cells from living RTT patients. We decided to use an alternative experimental model to study in vitro neurogenesis with biological samples obtained from RTT patients. In our opinion, MSCs could be a good alternative. Indeed, several groups demonstrated that MSCs can be induced to differentiate

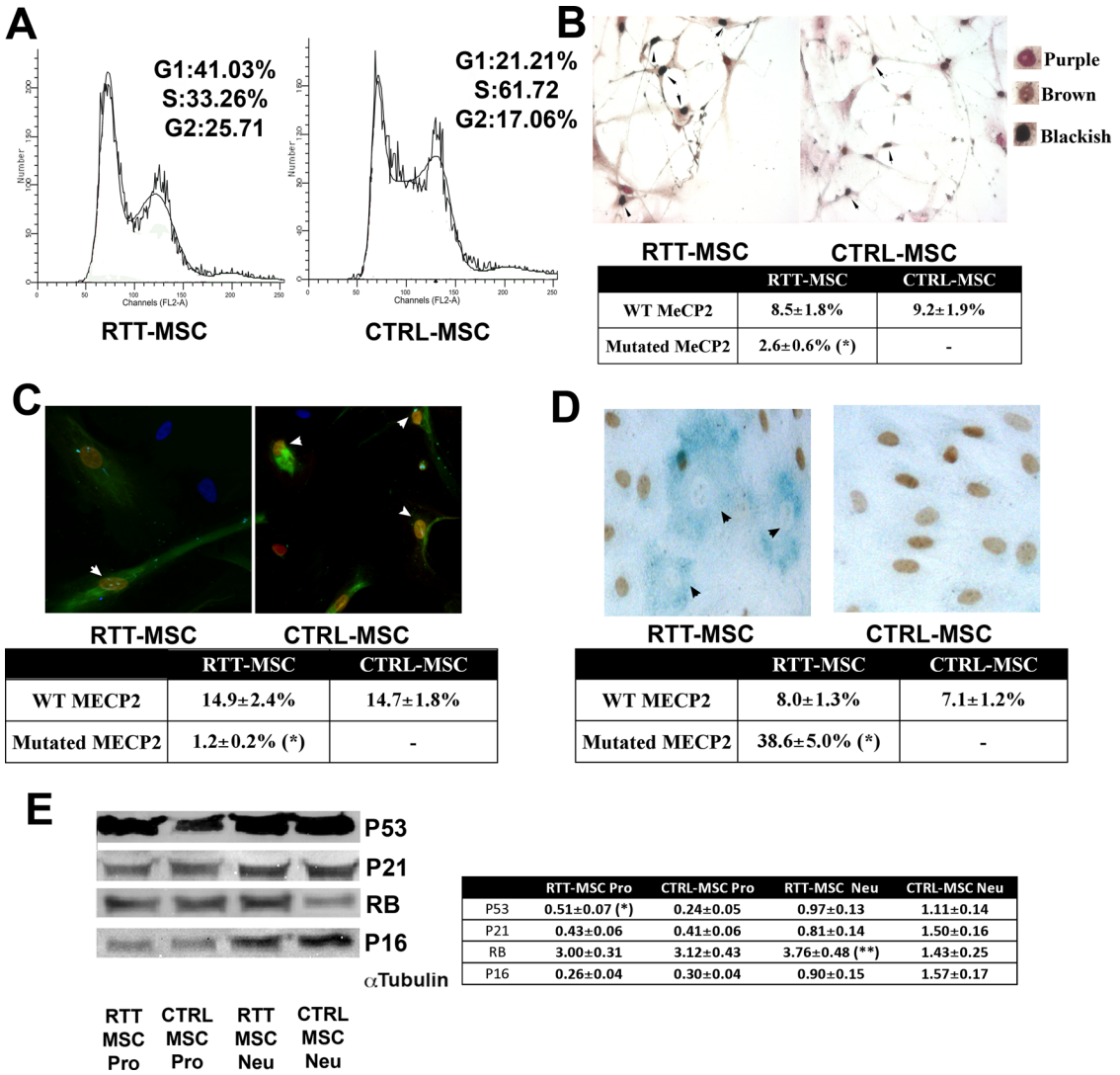

	RTT-MSC	CTRL-MSC
WT MeCP2	8.5±1.8%	9.2±1.9%
Mutated MeCP2	2.6±0.6% (*)	-

	RTT-MSC	CTRL-MSC
WT MECP2	14.9±2.4%	14.7±1.8%
Mutated MECP2	1.2±0.2% (*)	-

	RTT-MSC	CTRL-MSC
WT MECP2	8.0±1.3%	7.1±1.2%
Mutated MECP2	38.6±5.0% (*)	-

	RTT-MSC Pro	CTRL-MSC Pro	RTT-MSC Neu	CTRL-MSC Neu
P53	0.51±0.07 (*)	0.24±0.05	0.97±0.13	1.11±0.14
P21	0.43±0.06	0.41±0.06	0.81±0.14	1.50±0.16
RB	3.00±0.31	3.12±0.43	3.76±0.48 (**)	1.43±0.25
P16	0.26±0.04	0.30±0.04	0.90±0.15	1.57±0.17

FIGURE 1: Biological properties of MSCs from a RTT patient. (A) Flow cytometry analysis. Representative FACS profiles are shown of MSCs from a RTT patient (RTT-MSC) and from healthy controls (CTRL-MSC). Mean expression values are shown in the figure. The asterisk indicates statistically significant differences ($p < 0.05$) between RTT-MSC and control. (B) BrdU assay. The micrograph shows a representative field of BrdU (brown) and MECP2 (purple) staining in RTT-MSC and in CTRL-MSC. Double-labeled cells appear black. The arrows indicate double-labeled cells. The table shows the mean expression values and SDs ($n = 3$). The asterisk indicates statistically significant differences ($p < 0.05$) among mutated-MECP2 and wild-type cells in the RTT patient with respect to control MSCs. Right, are examples of brown-, purple-, and black-stained cells. (C) Annexin assay. The fluorescence photomicrograph shows cells stained with annexin V (green) and MECP2 (red) in RTT-MSC and in CTRL-MSC. Nuclei were counterstained with Hoechst 33342 (blue). The table shows the mean expression values of apoptotic cells (±SD, $n = 3$). The asterisk indicates statistically significant differences ($p < 0.05$) among mutated-MECP2 and wild-type cells in the RTT patient with respect to control MSCs. Arrows indicate double-labeled (annexin-MECP2) cells. (D) Senescence assay. A representative microscopic field of acid β-galactosidase (blue) and MECP2 (brown) staining in RTT-MSCs and in CTRL-MSCs. Arrows indicate MECP2-mutated cells that were β-galactosidase positive. The table shows the percentage of senescent cells (±SD, $n = 3$). The asterisk indicates statistically significant differences ($p < 0.05$) among mutated-MECP2 and wild-type cells in RTT patient with respect to control MSCs. (E) Western blot analysis of RB- and P53-related pathways in proliferating and differentiated MSCs from RTT patient and controls. Proliferating cells are named RTT-MSC Pro and CTRL-MSC Pro, and differentiated cells are RTT-MSC Neu and CTRL MSC Neu. Protein levels were normalized against α-tubulin, the loading control. The table shows the mean protein expression values (±SD, $n = 3$; *$p < 0.05$; **$p < 0.01$).

into neurons (Pittenger *et al.*, 1999; Woodbury *et al.*, 2000; Jori *et al.*, 2004, 2005a, 2005b).

Neural differentiation of MSCs occurred mainly in vitro, and their in vivo contribution to neurogenesis is negligible. Nevertheless, they might represent a tool with which to study the early phases of neural commitment and differentiation.

We investigated the process of in vitro neural differentiation by defining the expression patterns of genes representing "generic" neural differentiation and those associated with specific neurotransmission. To achieve this goal, we induced neural differentiation in MSCs using an advanced neural differentiation medium (see *Materials and Methods*) that contains a proprietary formulation of

growth factors. Morphological and molecular analyses of MSCs from the RTT patient and controls that displayed a neuron-like phenotype were performed.

We identified differentiating neurons by anti-NeuN immunostaining. In the proliferation medium, cells from healthy donors showed a lack of NeuN expression, but after 4 d of incubation in the neural induction medium, 41.7% (± 6.1%) of cells became positive for NeuN. In the RTT patient, this percentage did not change significantly in cells expressing wild-type MECP2. Conversely, the percentage of NeuN-positive cells was lower ($p < 0.05$) in the population bearing mutated MECP2 (Figure 2B and magnification of Figure 2B in Supplemental File 5). These data suggest that the mutation of MeCP2 results in a cell autonomous effect, in agreement with other reports showing that MeCP2 functions are largely cell autonomous in neuronal maturation (Kishi and Macklis, 2010).

As expected, differentiating cells were mainly in the G_1/G_0 cell cycle phase, and no significant differences were detected between neuron-like cultures from controls and those from the RTT patient (Figure 2A). FACS analysis was carried out on the whole population of MSCs from the RTT patient, and this would not us allow to detect minimal differences in cell cycle profile between wild-type and mutated-MECP2 subpopulations.

In progenitor cells (NeuN negative) from RTT patients, the percentage of apoptosis did not change significantly in cells expressing wild-type MECP2 as compared with the control (Figure 2C and magnification of Figure 2C in Supplemental File 6). In contrast, the percentage of apoptosis was lower ($p < 0.05$) in the population with mutated MECP2 (Figure 2C).

In neuron-like (NeuN-positive) cells from RTT patients, irrespective of MECP2 status, the apoptosis level was similar to that observed in the control sample (Figure 2C).

Differentiating MSCs from mutated MECP2s showed an increased percentage ($p < 0.05$) of senescent cells as compared with those from controls (Figure 2D). Increased senescence was observed both in the undifferentiated (NeuN-negative) and the differentiated (neuron-like) cell populations (Figure 2D).

In neuron-like cells from RTT patients, we detected a highly significant up-regulation ($p < 0.01$) of the pRb protein level as compared with the control sample (Figure 1E). In contrast, we did not find a significant modification of $p21^{Cip1}$, p53, and $p16^{INK4a}$ protein expression (Figure 1E).

Reverse transcription (RT)-PCR was used to analyze the expression of generic neuron differentiation markers such as neuron-specific enolase (NSE) and microtubule-associated protein 2 (MAP2; Pittenger *et al.*, 1999; Woodbury *et al.*, 2000; Jori *et al.*, 2004, 2005a, 2005b). MSC differentiation in neuron-like cells was associated with increased expression levels of both markers. MSCs differentiated from the RTT patient displayed a significant reduction ($p < 0.05$) of the expression of NSE and MAP2 compared with those differentiated from controls (Figure 2E). The observed decrease should be considered to be highly significant because RNA analysis was carried out on the whole population of MSCs from the RTT patient containing wild-type MECP2 cells, which differentiated normally.

Differentiated MSCs acquired a generic neuronal phenotype; we did not detect the expression of markers specific for cholinergic (acetylcholinesterase [ACHE]), dopaminergic (dopamine transporter [DAT]), noradrenergic (dopamine β-hydroxylase [DBH]), or serotonergic (tryptophan hydroxylase [TH]) neurons.

The senescence and reduced expression levels of neural markers in proliferating and differentiating MSCs from the RTT patient suggest that reduced activity of MECP2 protein, as observed in RTT patients, might impair neural commitment and differentiation.

In vitro neural differentiation of MSCs from patient with "fruste" RTT syndrome

To confirm and extend our data, we analyzed neural differentiation of MSCs obtained from a patient with the clinical manifestations of "fruste" Rett syndrome. She carried a de novo mutation (c. 1164–1207del) in the *MECP2* gene (Supplemental File 1).

In addition, in this patient, neural differentiation of MSCs was impaired as compared with the control. The percentage of neuron-like cells (NeuN-positive) was lower ($p < 0.05$) in the population bearing the mutated MECP2 (Supplemental File 2A).

This result was in agreement with RT-PCR experiments. MSCs differentiated from the RTT patient displayed a highly significant reduction ($p < 0.01$) of the expression of NSE as compared with those differentiated from controls (Supplemental File 2B).

MSCs with a mutated MECP2 showed an increased percentage of senescent cells ($p < 0.05$) as compared with those from controls (Supplemental File 2C). Increased senescence was observed both in the undifferentiated (NeuN-negative) and the differentiated (neuron-like) cell populations (Supplemental File 2C).

MECP2 silencing

The paucity of biological samples available from RTT patients permits limited analyses. To extend our findings, we studied neural differentiation in a human SK-N-BE(2)-C neuroblastoma cell line in which *MECP2* was silenced. This model is convenient for studies investigating neural progenitor cells. The neuroblastoma cell line was derived from human malignant neural crest cells (de Bernardi *et al.*, 1987) and shows an intermediate (I) phenotype that has been demonstrated to represent a multipotent embryonic stem cell of the peripheral nervous system. Therefore neuroblastoma cells can be induced to differentiate toward the committed neuronal N-type and glial S-type cells (Ciccarone *et al.*, 1989; Ross *et al.*, 1995; Jori *et al.*, 2001). To assess whether *MECP2* inactivation affected cell fate decisions of neural progenitors and/or neuronal differentiation and maintenance, to study different cell populations, we used the RheoSwitch Mammalian Inducible Expression System to silence *MECP2* in neuroblastoma cells before and after the induction of neural differentiation via retinoic acid treatment. In the first case, we evaluated the effects on multipotent embryonic precursor cells, and in the latter case, we performed the analysis using committed and neuronal-like cells.

The MECP2 gene is composed of four exons. Two alternatively spliced transcripts have been characterized: MECP2A (also called MECP2_E2) and MECP2B (also called MECP2_E1). The E1 isoform is composed of exons 1, 3, and 4, whereas the E2 isoform is composed of exons 1–4 (Singh *et al.*, 2008). To design hairpin small interfering RNAs (siRNAs), we selected several target regions that were present in both isoforms. All experiments were carried out with pNEBR-X1-MECP2-1706, which targets nucleotides (nt) 1706–1724 of MECP2 mRNA (GenBank accession number NM_004992.3). In a previous study, we demonstrated the effectiveness of such hairpin siRNA, which we transduced in cell cultures by adenoviral vectors (Squillaro *et al.*, 2010). Confirmatory experiments were carried out with pNEBR-X1-MECP2-4398 and pNEBR-X1-MECP2-1229, which target nt 4398–4416 and 1229–1247, respectively (see later discussion).

Proliferating neuroblastoma cells were cotransfected with pNEBR-R1 (regulator plasmid) and either pNEBR-X1-MECP2-1706 or pNEBR-X1-CTRL carrying short hairpin RNAs (shRNAs). The R1 plasmids contained the hygromycin B gene, whereas the X1 plasmid had the G418 gene. These antibiotic resistance genes were used for generation of stable cell lines.

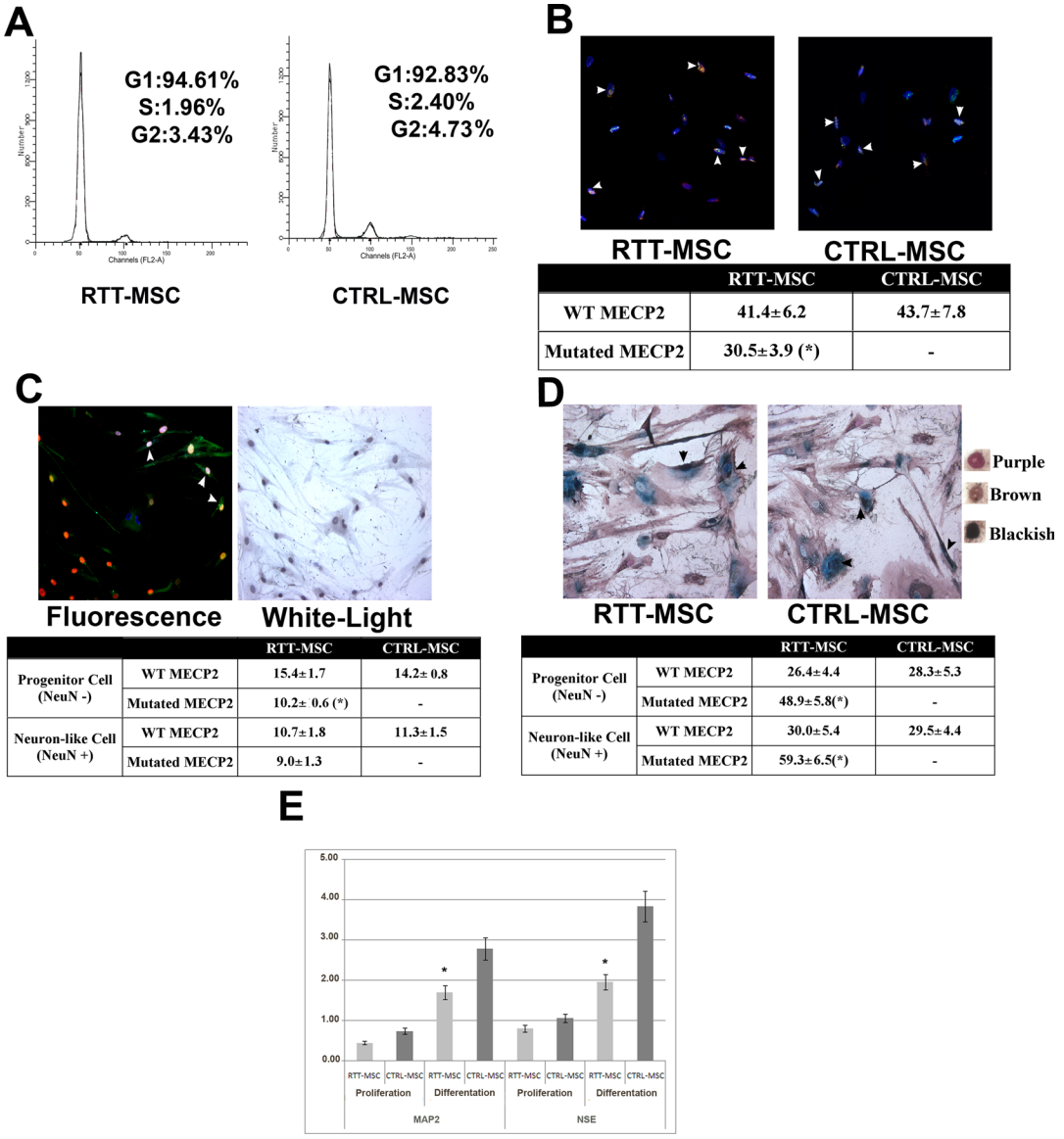

	RTT-MSC	CTRL-MSC
WT MECP2	41.4±6.2	43.7±7.8
Mutated MECP2	30.5±3.9 (*)	-

		RTT-MSC	CTRL-MSC
Progenitor Cell (NeuN -)	WT MECP2	15.4±1.7	14.2± 0.8
	Mutated MECP2	10.2± 0.6 (*)	-
Neuron-like Cell (NeuN +)	WT MECP2	10.7±1.8	11.3±1.5
	Mutated MECP2	9.0±1.3	-

		RTT-MSC	CTRL-MSC
Progenitor Cell (NeuN -)	WT MECP2	26.4±4.4	28.3±5.3
	Mutated MECP2	48.9±5.8(*)	-
Neuron-like Cell (NeuN +)	WT MECP2	30.0±5.4	29.5±4.4
	Mutated MECP2	59.3±6.5(*)	-

FIGURE 2: Neural differentiation of MSCs from a RTT patient. (A) Flow cytometry analysis. Representative FACS profiles of RTT patient stem cells (RTT-MSC) and healthy control stem cells (CTRL-MSC) following neural differentiation. (B) NeuN staining. Fluorescence photomicrograph shows representative fields of cells stained with NeuN (red) and MECP2 (green) in differentiated RTT-MSC and CTRL-MSC. Nuclei were counterstained with Hoechst 33342 (blue). Arrows indicate double-labeled (NeuN-MECP2) cells. The table shows the mean expression percentages of NeuN-positive cells (± SD, n = 3). Statistical analysis was carried out comparing the same cell type among mutated-MECP2 and wild-type cells in the RTT patient with respect to control MSCs. The z indicates statistical differences ($p < 0.05$). Supplemental File 5 shows B in higher magnification. (C) Annexin assay in differentiated MSCs. The representative fluorescence photomicrograph shows cells stained with annexin V (green), NeuN (blue), and MECP2 (red). Light microscopy picture shows the same field with hematoxylin-stained nuclei. The differentiation procedure was performed both in RTT-MSC and in CTRL-MSC. Arrowheads indicate triple (NeuN–annexin V–MECP2)–positive cells. The table shows the percentage of apoptotic cells for each cell type (±SD, n = 3). Supplemental File 6 shows C in higher magnification. Statistical analysis was carried out comparing the same cell type among mutated-MECP2 and wild-type cells in the RTT patient with respect to control MSCs. The asterisk indicates statistically significant differences ($p < 0.05$). (D) Senescence assay in differentiated MSCs. The photomicrographs show acid β-galactosidase–positive cells (blue) and cells stained with NeuN (brown) and MECP2 (purple). Double-labeled cells (NeuN-MECP2) appear black. The differentiation procedure was performed both in RTT-MSC and in CTRL-MSC. Arrowheads indicate triple (NeuN–β-galactosidase–MECP2)–positive cells. Right, examples of brown-, purple-, and black-stained cells. The table shows the percentage of senescent cells for each cell type (±SD, n = 3). Statistical analysis was carried out comparing the same cell type among mutated-MECP2 and wild-type cells in the RTT patient with respect to control MSCs. The asterisk indicates statistically significant differences ($p < 0.05$). (E) Expression analysis of neural differentiation markers by RT-PCR. The mRNA levels were normalized to HPRT as an internal control. The histogram shows the mean expression values (±SD, n = 3) of NSE and MAP2 in both proliferating and in differentiated MSCs. Statistical analysis was carried out comparing the same cell type among the RTT patient with respect to control MSCs. The asterisk indicates statistically significant differences ($p < 0.05$). The comparative cycle threshold method was used for quantitative analysis.

On addition of the synthetic RSL1 ligand to the culture medium, the RheoReceptor and the RheoActivator proteins stably dimerized and bound to the response element of the pNEBR-R1 plasmids. This process, in turn, activated shRNA transcription and silenced MECP2 expression, as detected by RT-PCR using a primer pair that identified both isoforms (Figure 3A). The specific down-regulation of each isoform was evaluated with a semiquantitative RT-PCR, since primer pairs that distinguish the two isoforms were not suitable for real-time RT-PCR (Figure 3A). The silencing of MECP2 was observed in almost all cells in the culture because the antibiotic treatment selected only cells stably expressing the hairpin siRNAs (unpublished data).

Next, in cells with silenced MECP2 and in controls, we induced neural differentiation by incubating cultures for 7 d with retinoic acid. Of note, the percentage of neurons was greatly reduced ($p < 0.05$) in cells that demonstrated decreased *MECP2* expression compared with control cultures, as detected by NeuN immunostaining (18.6 vs. 37.9%; Figure 3B). This reduction was associated with a decreased number of BrdU-positive cells (Figure 3C). Moreover, MECP2 down-regulation augmented ($p < 0.05$) the percentage of senescent cells both in uncommitted/undifferentiated (NeuN-negative) and neuronal-like (NeuN-positive) populations (Figure 3D).

Senescence was associated with a decrease in the percentage ($p < 0.05$) of apoptotic cells in uncommitted/undifferentiated cells (Figure 3E). This finding suggests that the reduced percentage of neuronal-like cells observed in *MECP2*-silenced cultures may be attributed to the senescence of neural precursors rather than to cell death either in uncommitted cells or in neuronal-like cells (Figure 3E).

In a second group of experiments, we induced neural differentiation in neuroblastoma cells that were stably cotransfected with pNEBR-R1 (regulator plasmid) and either pNEBR-X1-MECP2-1706 or pNEBR-X1-CTRL carrying shRNAs. Three days after retinoic acid treatment, RSL1 ligand was added to the cultures, and the cultures were incubated for an additional 4 d in differentiation medium.

At the end of this period, we assessed MECP2 mRNA levels and found that they were decreased ($p < 0.01$) in cells treated with pNEBR-X1-MECP2-1706 compared with those treated with the control plasmid, as expected (Figure 4A). Partial silencing of MECP2 in cells following the induction of neural differentiation did not affect the percentage of NeuN-positive cells (Figure 4B). These results indicate that MECP2 silencing after cell commitment does not modify the number of neurons.

MECP2 silencing enhanced the cell proliferation arrest observed in neural differentiation medium. MECP2 down-regulation induced an increase ($p < 0.05$) in senescent cells (Figure 4C). Of great interest, the percentage of senescent differentiated neurons more than doubled (38 vs. 16%) in cells that carried partially silenced MECP2 compared with control cells (Figure 4C). The down-regulation of MECP2 following neural induction also increased ($p < 0.05$) senescence in uncommitted/undifferentiated cells (Figure 4C). These data are consistent with results obtained when MECP2 was silenced before the induction of neural differentiation.

Senescence was associated with a decrease ($p < 0.05$) in the percentage of apoptotic cells in uncommitted/undifferentiated cells and in neuronal-like cells (Figure 4D).

The biological effects we detected in neuroblastoma cells with a silenced MECP2 through treatment with hairpin siRNA MECP2-1706 might be not specifically related to MECP2 down-regulation.

To rule out the off-target effects of hairpin siRNA-1706, we also transfected neuroblastoma cells with pNEBR-X1-MECP2-4398 and pNEBR-X1-MECP2-1229. Both hairpin siRNAs induced silencing of the MECP2 gene (Supplemental File 3A).

We selected pNEBR-X1-MECP2-4398 for further experiments. In cells with a silenced MECP2 through pNEBR-X1-MECP2-4398 and in controls, we induced neural differentiation by incubating cultures for 7 d with retinoic acid. It is worth noting that as detected with hairpin siRNA MECP2-1706, the percentage of neurons was greatly reduced ($p < 0.05$) in cells with decreased *MECP2* expression as compared with control cultures (Supplemental File 3B).

In addition, siRNA-4398 augmented the percentage of senescent cells both in uncommitted/undifferentiated ($p < 0.05$) and neuronal-like cell populations and decreased the percentage of apoptotic cells in uncommitted/undifferentiated cells (Supplemental File 3C).

DISCUSSION

Although mutations in the MECP2 gene are associated with RTT syndrome, the role of MECP2 in this disease remains unknown. MECP2 displays complex spatial and temporal distribution patterns. MECP2 expression is high in the brain—specifically in neurons rather than glia. Nevertheless, MECP2 expression can be detected in the majority of the body tissues (Bienvenu and Chelly, 2006; Singh *et al.*, 2008). Thus it is not clear why MECP2 dysfunctions affect only neural cells in RTT patients.

Several mouse models have been used to address the role of MECP2 in brain development and maturation and in the mechanisms that underlie RTT syndrome. These transgenic mice displayed a RTT-like phenotype, but the researchers did not obtain a clear pathological or molecular understanding of the abnormalities present in the brain.

Other studies attempted to investigate global gene expression changes in the brain tissues of mice lacking MECP2 and in RTT patients. These studies documented conflicting results, and only a few genes were identified as MECP2 targets (Bienvenu and Chelly, 2006).

Finally, some findings were focused strictly on the role of MECP2 during neural cell commitment, differentiation, and maintenance. Expression studies in a RTT mouse model suggested that MECP2 was involved in the differentiation of neuronal cells rather than in cell fate decisions (Kishi and Macklis, 2004). In contrast, in a *Xenopus* embryo model, the lack of MECP2 affected neural cell fates (Stancheva *et al.*, 2003). In addition to these discrepancies, it should be noted that animal models do not completely recapitulate the pathogenesis of human disease.

Another caveat arises from "restrictive studies" on RTT syndrome. RTT is a neurodevelopmental disease, and hence studies examining the phenotype of RTT patients and animal models have focused primarily on neuronal functions. Therefore more subtle deficiencies that are unrelated to neural activities and/or impairment of cell functions outside of the nervous system may have been overlooked.

In our previous work, we showed that MSCs obtained from RTT patients are prone to senescence in comparison with wild-type cells. These data were confirmed in an in vitro model of partial MECP2 silencing (Squillaro *et al.*, 2008c, 2010).

In the present study, we sought to verify whether senescence induced by reduced MECP2 activity could affect the cell fate decisions of neural progenitors and/or neuronal differentiation and maintenance.

To achieve this goal, we assessed the neural differentiation process in MSCs obtained from a RTT patient and from healthy donors. We further analyzed neural differentiation in a human neuroblastoma cell line carrying a partially silenced MECP2 gene before and after the induction of in vitro differentiation.

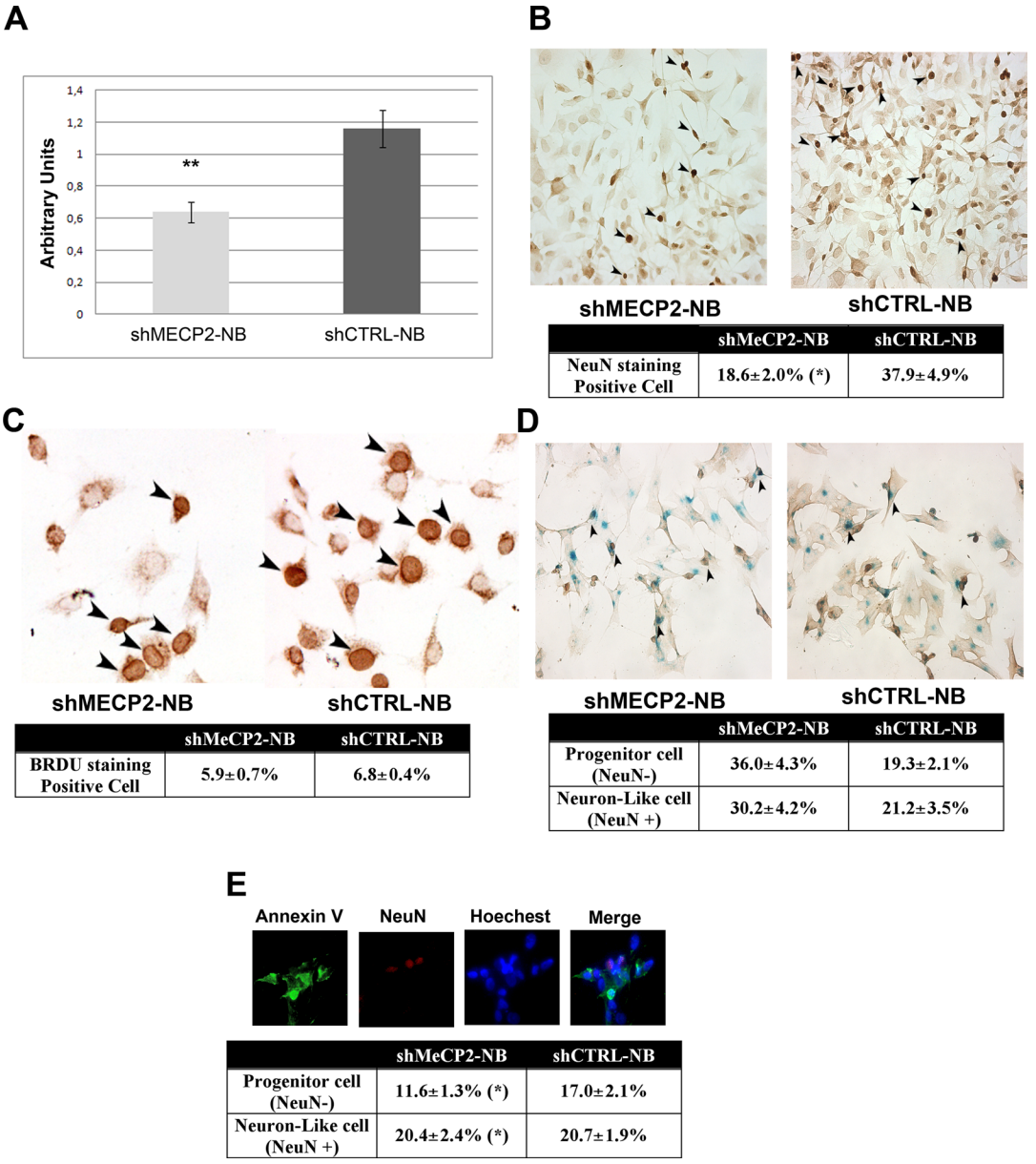

	shMeCP2-NB	shCTRL-NB
NeuN staining Positive Cell	18.6±2.0% (*)	37.9±4.9%

	shMeCP2-NB	shCTRL-NB
BRDU staining Positive Cell	5.9±0.7%	6.8±0.4%

	shMeCP2-NB	shCTRL-NB
Progenitor cell (NeuN-)	36.0±4.3%	19.3±2.1%
Neuron-Like cell (NeuN +)	30.2±4.2%	21.2±3.5%

	shMeCP2-NB	shCTRL-NB
Progenitor cell (NeuN-)	11.6±1.3% (*)	17.0±2.1%
Neuron-Like cell (NeuN +)	20.4±2.4% (*)	20.7±1.9%

FIGURE 3: Effects of MECP2 silencing before neural differentiation. (A) MECP2 silencing in proliferating neuroblastoma cells. To induce shRNA transcription, the synthetic RSL1 ligand was added to SK-N-BE(2)-C cell cultures that had been cotransfected with pNEBR-R1 (regulator plasmid) and either pNEBR-X1-MECP2 or pNEBR-X1-CTRL. MECP2 silencing was assessed by RT-PCR. The mRNA levels were normalized to HPRT as an internal control. The histogram shows the mean expression values of mRNA levels (±SD, n = 3, **p < 0.01). The comparative cycle threshold method was used for the quantitative analysis. Neuroblastoma cells expressing MECP2 shRNA are indicated as shMECP2-NBs, and cells expressing control shRNA are indicated as shCTRL-NBs. (B) NeuN staining to assess neural differentiation in cells with silenced MECP2. The photomicrograph shows representative fields of cells stained with NeuN (dark brown) in differentiated shMECP2-NBs and in shCTRL-NBs. Arrowheads indicate NeuN-positive cells. The table shows the mean expression values of NeuN-positive and -negative cells (±SD, n = 3; *p < 0.05). (C) BrdU assay. Photomicrograph shows a representative field of BrdU incorporation in shMECP2-NBs and shCTRL-NBs. Arrowheads indicate BrdU-positive cells. The table shows the mean expression values of BrdU-positive cells (±SD, n = 3). (D) Senescence assay in MECP2-silenced neuroblastoma cells that were induced to differentiate into neuronal-like cells. The photomicrographs show acid β-galactosidase-positive (blue) and NeuN-positive (brown) cells. Arrowheads indicate double (NeuN, β-galactosidase)–positive cells. The differentiation procedure was performed in both shMECP2-NBs and shCTRL-NBs. The table shows the percentage of senescent cells in the undifferentiated (NeuN-negative) and neuronal-like (NeuN-positive) populations (±SD, n = 3). The asterisk indicates statistically significant differences (p < 0.05) between the same cell type in samples with silenced MECP2 and control. (E) Annexin assay in MECP2-silenced neuroblastoma cells that were induced to differentiate into neuronal-like cells. The fluorescence photomicrographs show cells stained with annexin V (green) and NeuN (red). Nuclei were counterstained with Hoechst 33342. The differentiation procedure was performed in both shMECP2-NBs and shCTRL-NBs. A representative field is shown. The table shows the percentage of apoptotic cells in the undifferentiated (NeuN-negative) and neuronal-like (NeuN-positive) populations (±SD, n = 3). The asterisk indicates statistically significant differences (p < 0.05) between the same cell type in samples with silenced MECP2 and control.

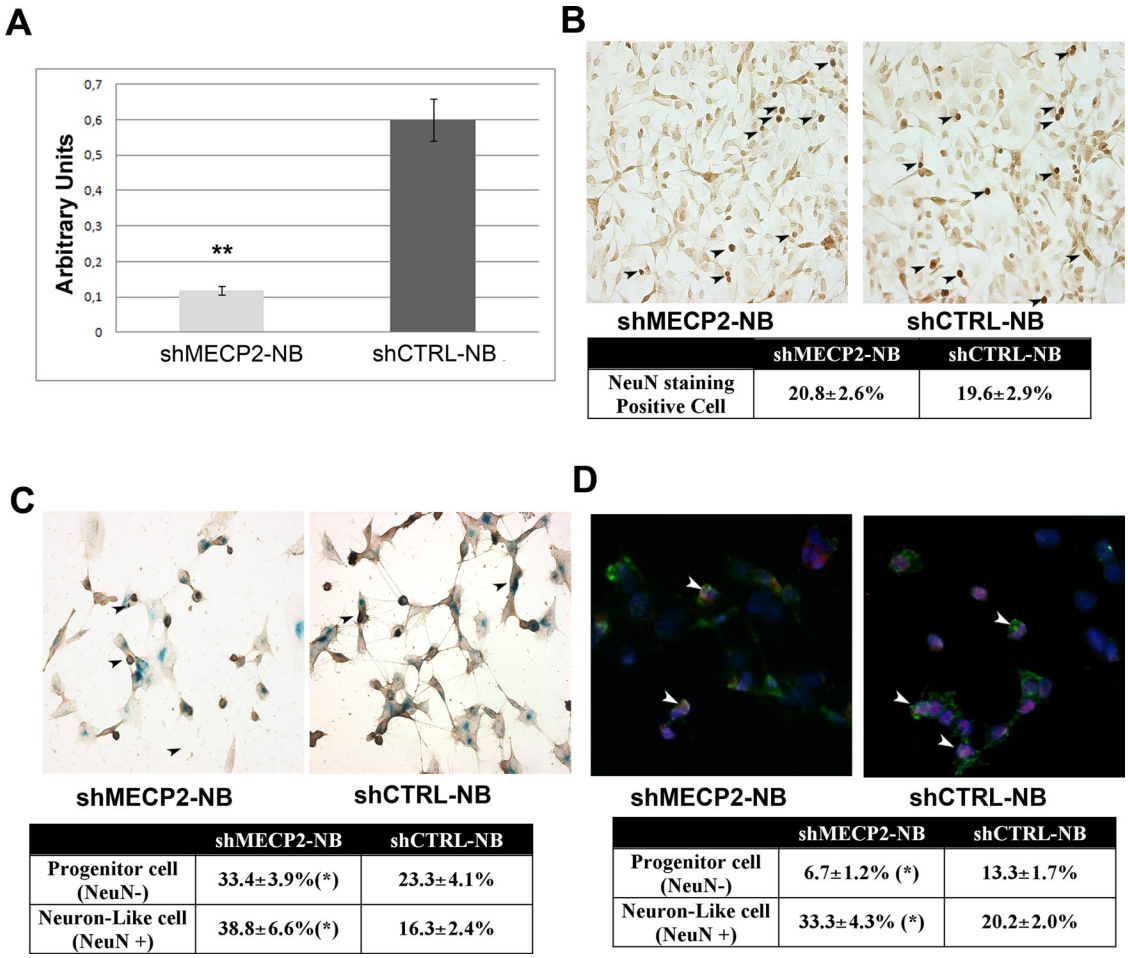

	shMECP2-NB	shCTRL-NB
NeuN staining Positive Cell	20.8±2.6%	19.6±2.9%

	shMECP2-NB	shCTRL-NB
Progenitor cell (NeuN-)	33.4±3.9%(*)	23.3±4.1%
Neuron-Like cell (NeuN +)	38.8±6.6%(*)	16.3±2.4%

	shMECP2-NB	shCTRL-NB
Progenitor cell (NeuN-)	6.7±1.2% (*)	13.3±1.7%
Neuron-Like cell (NeuN +)	33.3±4.3% (*)	20.2±2.0%

FIGURE 4: Effects of MECP2 silencing after neural differentiation. (A) MECP2 silencing in differentiated neuroblastoma cells. To induce shRNA transcription, the synthetic RSL1 ligand was added to SK-N-BE(2)-C cell cultures that had been cotransfected with pNEBR-R1 (regulator plasmid) and either pNEBR-X1-MECP2 or pNEBR-X1-CTRL. MECP2 silencing was assessed by RT-PCR. The mRNA levels of MECP2 were normalized to hypoxanthine phosphoribosyltransferase as an internal control. The histogram shows the mean expression values (±SD, n = 3; **$p < 0.01$). The comparative cycle threshold method was used for the quantitative analysis. Neuroblastoma cells expressing MECP2 shRNA are indicated as shMECP2-NBs, and cells expressing control shRNA are indicated as shCTRL-NBs. (B) NeuN staining to evaluate neural differentiation in cells with silenced MECP2. The photomicrograph shows representative fields of cells stained with NeuN (dark brown) in differentiated RTT-MSCs and in CTRL-MSCs. Arrowheads indicate NeuN-positive cells. The table shows the mean expression values of NeuN-positive and -negative cells (±SD, n = 3). (C) Senescence assay. The photomicrographs show acid β-galactosidase–positive (blue) and NeuN-positive (brown) cells. The differentiation procedure was performed both in shMECP2-NBs and in shCTRL-NBs. Arrowheads indicate double (NeuN, β-galactosidase)–positive cells. The table shows the percentage of senescent cells for each cell type (±SD, n = 3). The asterisk indicates statistically significant differences ($p < 0.05$) between the same cell type in samples with silenced MECP2 and control. (D) Annexin assay. The fluorescence photomicrographs show cells stained with annexin V (green) and NeuN (red). Nuclei were counterstained with Hoechst 33342. The differentiation procedure was performed both in shMECP2-NBs and in shCTRL-NBs. Arrowheads indicate double (NeuN, annexin V)–positive cells. The table shows the percentage of apoptotic cells for each cell type (±SD, n = 3). The asterisk indicates statistically significant differences ($p < 0.05$) between the same cell type in samples with silenced MECP2 and control.

In proliferating and differentiating MSCs from the RTT patient, senescence and decreased expression levels of neural markers were observed in cells expressing mutated MECP2, which suggests that the reduced activity of MECP2 protein, as observed in RTT patients, may impair neural differentiation via a mechanism that is mediated by senescence (Figure 2, A–E).

Silencing experiments in a neuroblastoma cell line allowed us to better determine the role of MECP2 during neural cell development. MECP2 expression was down-regulated in two different temporal windows (before and after the induction of neural differentiation) to study different cell populations. In the first case, we evaluated the effects on multipotent embryonic precursor cells, and in the latter case, we performed the analysis using committed and neuronal-like cells.

Our results suggest that the reduced activity of MECP2 induces a decrease in cell proliferation and triggers senescence in neural precursor cells. This process in turn could impair neural cell formation (Figure 3, A–C).

The diminished MECP2 activity also seemed to affect the functions of committed and neuronal-like cells, as indicated by the

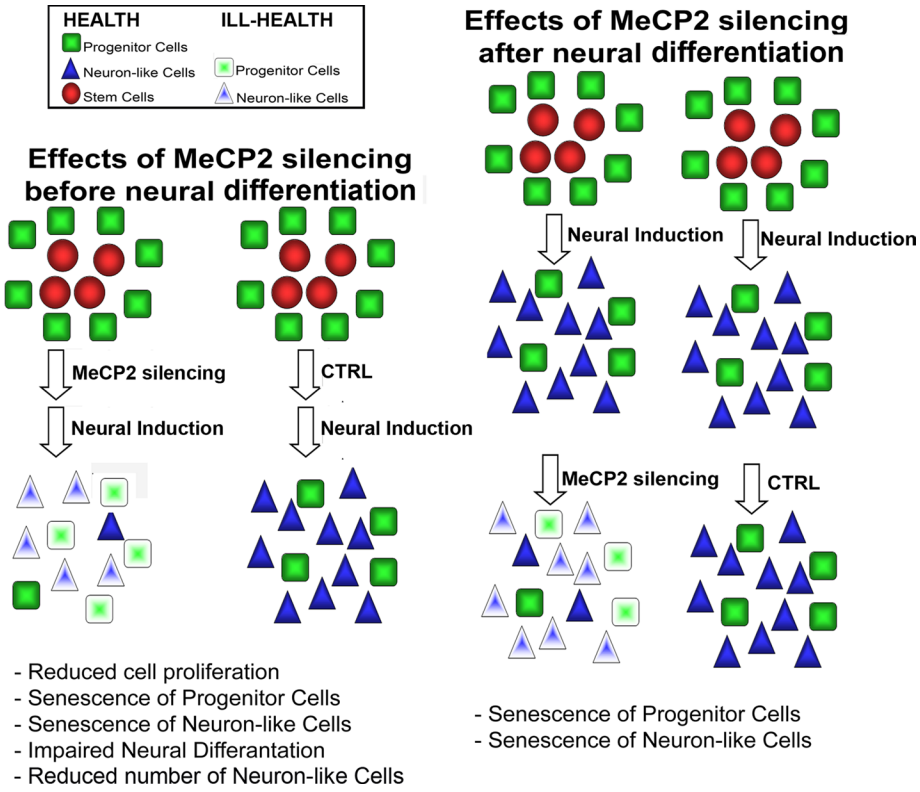

FIGURE 5: Effects of MECP2 silencing in a simplified model of neurogenesis. Under proliferative conditions, neuroblastoma cultures consist of stem cells (red ovals) and progenitors (green squares). Following neural differentiation, the pool of stem cells is committed toward progenitors, which differentiate into neuronal-like cells (blue triangles). Left, MECP2 gene expression was silenced in proliferating neuroblastoma cells, and the cells were induced to differentiate into neuronal-like cells. Right, neuroblastoma cells were differentiated into neuronal-like cells, and MECP2 expression in the cells was then silenced.

decreased cell growth observed in committed cells and the increased percentage of senescent cells detected both in committed and in neuronal-like cells (Figure 4).

In conclusion, our data suggest that neural cell fate decisions and neuronal maintenance may be perturbed by the senescence triggered by impaired MECP2 activity either before or after neural differentiation (Figure 5). Our data are in good agreement with a recent article showing that neuronal maturation is impaired in induced pluripotent stem cells from patients with Rett syndrome (Kim *et al.*, 2011).

To our knowledge, this is the first study to identify an association between RTT syndrome and senescence and the impairment of neural development and differentiation. These studies may shed new light on the dysfunctions associated with impaired MECP2 activity that lead to RTT syndrome.

MATERIALS AND METHODS

Molecular analysis of the identified patient

Blood samples were collected after informed consent was obtained. DNA was extracted from peripheral blood using a QIAamp DNA Blood Kit (Qiagen, Milan, Italy). DNA samples were screened for mutations in the four exons coding for *MECP2* using transgenomic WAVE denaturing high-performance liquid chromatography (DHPLC). Analysis of the *MECP2* gene for deletions/duplications was performed as previously described (Ariani *et al.*, 2004) and as indicated in Supplemental File 1. PCR products that provided abnormal DHPLC profiles were sequenced on both strands using PCR primers with fluorescent dye terminators on an ABI PRISM 310 genetic analyzer (PE Applied Biosystems, Foster City, CA).

MSC cultures

Bone marrow was collected from a girl with RTT syndrome and two healthy children after obtaining informed consent. The cells were separated on a Ficoll density gradient (GE Healthcare, Milan, Italy), and MSC cultures were obtained as described previously (Squillaro *et al.*, 2008c, 2010).

To induce neural differentiation, cells were plated on tissue culture dishes at ~2500 cells/cm^2 in proliferating medium. When the cells reached 30% confluence, the medium was discarded, the cell plates were washed with phosphate-buffered saline (PBS), and complete neural differentiation medium was added (Thermo Scientific, Waltham, MA). The formation of neuron-like cells was observed within 24 h and peaked at 72 h. To maintain cells in a differentiated state, we added additional neural differentiation medium every 48 h.

Neuroblastoma cell cultures

SK-N-BE(2)-C neuroblastoma cells were grown in monolayers and maintained at 37°C under 5% CO_2 in RPMI 1640 containing 10% fetal bovine serum, 2 mM L-glutamine, 50 U/ml penicillin, and 100 µg/ml streptomycin. To induce neural differentiation, 10^{-6} M all-*trans* retinoic acid (Sigma Aldrich, St. Louis, MO) was added to the culture medium for 7 d.

Silencing

Hairpin siRNAs targeted against human MECP2 mRNA (GenBank accession number NM_004992.3) were selected using the design algorithm developed by Cenix Bioscience (Dresden, Germany) on the basis of rules and criteria as already described (Pittenger *et al.*, 1999; Reynolds *et al.*, 2004).

We selected three target regions of MECP2 mRNA to design hairpin siRNAs:

5′-GCAAAGCAAACCAACAAGA-3′ (nt 1706–1724)
5′-GGTTGTCACTGAGAAGATG-3′ (nt 4398–4416)
5′-GGACTGAAGACCTGTAAGA-3′ (nt 1229–1247)

The siRNA negative control was as described (Harborth *et al.*, 2001) and targets the firefly (*Photinus pyralis*) luciferase gene (GenBank accession number X65324). The negative control siRNA exhibits no target mRNA in the human transcriptome.

For each hairpin siRNA, we designed two complementary oligonucleotides (55-mers); each included the 19-mer siRNA in sense orientation, followed by the loop sequence 5′-TTCAAGAGA-3′ and by the 19-mer siRNA in antisense orientation. The 5′ ends of the two oligonucleotides had *Xho*I and *Bam*HI restriction site overhangs to facilitate the efficient directional cloning into the pNEBR-X1 plasmid (see later discussion).

The complementary hairpin siRNA template oligonucleotides were synthesized (MWG Biotech, Ebersberg, Germany) and then

were annealed to form a double-stranded DNA. The annealed siRNA template inserts were ligated into the pNEBR-X1 plasmid according the manufacturer's protocol and routine procedures for DNA cloning (Sambrook and Russell, 2001).

We cloned and produced four recombinant plasmids: pNEBR-X1-MECP2-1706; pNEBR-X1-MECP2-4398; pNEBR-X1-MECP2-1229, which targeted MECP2; and pNEBR-X1-CTRL, a control shRNA, which targeted the firefly luciferase gene.

Neuroblastoma cell cultures were cotransfected with pNEBR-R1 (regulator plasmid) and either pNEBR-X1-MECP2 plasmids or pNEBR-X1-CTRL.

The neomycin resistance gene in pNEBR1-R1 and the hygromycin resistance gene in the pNEBR-X1 plasmid were used to select stable cells growing in media containing 500 μg/ml G418 and 50 μg/ml hygromycin. Stable cell lines expressing the RheoReceptor and the RheoActivator proteins via pNEBR1-R1 were generated. In these cell lines, shRNA transcription was turned off under basal conditions. By adding the synthetic RSL1 ligand to culture medium, the RheoReceptor and the RheoActivator proteins were dimerized stably and bound to the response element of pNEBR-R1 plasmids. This in turn activated shRNA transcription.

Following the silencing of MECP2, the rescue of its expression was obtained via the removal of RSL1 ligand from the culture medium after cultivating the cells for 48 h.

Cell cycle analysis

For each assay, 3×10^5 cells were collected and resuspended in a hypotonic buffer containing propidium iodide. Cells were incubated in the dark and then analyzed. Samples were acquired using a FACSCalibur flow cytometer with CellQuest software (BD Biosciences, Franklin Lakes, NJ) and analyzed according to standard procedures with CellQuest and ModFitLT software (BD Biosciences).

Detection of MECP2 by immunocytochemistry

MECP2 was detected using the anti-MECP2 (clone Mec-168) primary antibody (Abcam, Cambridge, United Kingdom) according to the manufacturer's protocol. Cells were analyzed using either fluorescence or a light microscope. In the first case, the cells were incubated with goat anti-mouse secondary antibodies and conjugated to Texas red (Jackson ImmunoResearch Laboratories, West Grove, PA), and the nuclei were counterstained with Hoechst 33342. Alternatively, the cells were incubated with goat anti-mouse secondary antibodies, conjugated to peroxidase (Santa Cruz Biotechnology, Santa Cruz, CA), and then treated with the DAB substrate (Roche, Mannheim, Germany) or conjugated to alkaline phosphatase (Santa Cruz Biotechnology) and then treated with the Vector Red Alkaline Phosphatase Substrate Kit (Vector Laboratories, Burlingame, CA).

The percentage of MECP2-positive cells was calculated by counting at least 500 cells in different microscopic fields (see also Supplemental File 11).

BrdU assay

For BrdU immunostaining, the cells were grown on glass coverslips and incubated for 10 h with 10 μM BrdU (Sigma-Aldrich). Briefly, the cells were rinsed with PBS, fixed with 100% methanol at 4°C for 10 min, air dried, and then incubated with 2 N HCl for 60 min at 37°C. HCl was neutralized with 0.1 M borate buffer (pH 8.5). Following additional PBS washes, the slides were incubated with an anti-BrdU rabbit polyclonal antibody (1:200; Bioss, Woburn, MA). After 60 min at room temperature, the cells were washed with PBS and incubated with goat anti-rabbit secondary antibodies conjugated to peroxidase (Santa Cruz Biotechnology) for 60 min at room temperature. Finally, after additional washes in PBS, the slides were treated with DAB substrate (see also Supplemental File 11).

Detection of apoptotic cells

Apoptotic cells were detected using fluorescein-conjugated annexin V (Roche, Milan, Italy) according to the manufacturer's instructions. Apoptotic cells were observed using a fluorescence microscope (Leica Italia, Milan, Italy). In each experiment, at least 1000 cells were counted in different fields to calculate the percentage of dead cells in each culture (see also Supplemental File 11).

Senescence-associated β-galactosidase assay

The cells were fixed with a solution of 2% formaldehyde and 0.2% glutaraldehyde. The cells were then washed with PBS and incubated at 37°C for at least 2 h with a staining solution according to the manufacturer's protocol (Roche, Italy). The percentage of senescent cells was calculated based on the number of β-galactosidase–positive cells among at least 500 cells in different microscopic fields; see also Supplemental File 11).

Neuronal nuclei detection

NeuN was detected by immunocytochemistry using the anti-NeuN primary antibody (Millipore, Milan, Italy) according to the manufacturer's protocol. Cells were analyzed using either a fluorescence or a light microscope. In the first case, the cells were incubated with goat anti-rabbit secondary antibodies conjugated to tetramethylrhodamine isothiocyanate or aminomethylcoumarin acetate (Jackson ImmunoResearch Laboratories), and the nuclei were counterstained with Hoechst 33342. Alternatively, the cells were incubated with goat anti-rabbit secondary antibodies conjugated to peroxidase (Santa Cruz Biotechnology) and then treated with the appropriate substrate.

The percentage of NeuN-positive cells was calculated by counting at least 500 cells in different microscopic fields (see also Supplemental File 11).

RNA extraction, RT-PCR, and real-time PCR

Total RNA was extracted from cell cultures using Omnizol (Euroclone, Milan, Italy) according to the manufacturer's protocol. mRNA levels were measured by RT-PCR amplification as previously reported (Galderisi *et al.*, 1999). The primers used are listed in Supplemental File 4.

Real-time PCR assays were performed using an Opticon-4 machine (Bio-Rad, Hercules, CA). The reactions were performed according to the manufacturer's instructions using a SYBR green PCR Master Mix.

Western blotting

Cells were lysed in a buffer containing 0.1% Triton for 30 min at 4°C. The lysates were then centrifuged for 10 min at 10,000 × *g* at 4°C. After centrifugation, 10–40 μg of each sample was loaded electrophoresed in a polyacrylamide gel and electroblotted onto a nitrocellulose membrane. All the primary antibodies were used according to the manufacturers' instructions. Immunoreactive signals were detected with a horseradish peroxidase–conjugated secondary antibody (Santa Cruz Biotechnology) and reacted with ECL Plus reagent (GE Healthcare, Italy).

Statistical analysis

Statistical significance was evaluated by analysis of variance followed by Student's *t* test or Bonferroni test.

ACKNOWLEDGMENTS

This work was partially supported by Sbarro Health Research Organization funds to U.G. and A.G. We thank M. R. Cipollaro for technical assistance.

REFERENCES

Ariani F, Mari F, Pescucci C, Longo I, Bruttini M, Meloni I, Hayek G, Rocchi R, Zappella M, Renieri A (2004). Real-time quantitative PCR as a routine method for screening large rearrangements in Rett syndrome: report of one case of MECP2 deletion and one case of MECP2 duplication. Hum Mutat 24, 172–177.

Bienvenu T, Chelly J (2006). Molecular genetics of Rett syndrome: when DNA methylation goes unrecognized. Nat Rev Genet 7, 415–426.

Campisi J, d'Adda di Fagagna F (2007). Cellular senescence: when bad things happen to good cells. Nat Rev Mol Cell Biol 8, 729–740.

Chen RZ, Akbarian S, Tudor M, Jaenisch R (2001). Deficiency of methyl-CpG binding protein-2 in CNS neurons results in a Rett-like phenotype in mice. Nat Genet 27, 327–331.

Ciccarone V, Spengler BA, Meyers MB, Biedler JL, Ross RA (1989). Phenotypic diversification in human neuroblastoma cells: expression of distinct neural crest lineages. Cancer Res 49, 219–225.

de Bernardi B, Rogers D, Carli M, Madon E, de Laurentis T, Bagnulo S, di Tullio MT, Paolucci G, Pastore G (1987). Localized neuroblastoma. Surgical and pathologic staging. Cancer 60, 1066–1072.

Fuks F, Hurd PJ, Wolf D, Nan X, Bird AP, Kouzarides T (2003). The methyl-CpG-binding protein MeCP2 links DNA methylation to histone methylation. J Biol Chem 278, 4035–4040.

Galderisi U, Di Bernardo G, Cipollaro M, Peluso G, Cascino A, Cotrufo R, Melone MA (1999). Differentiation and apoptosis of neuroblastoma cells: role of N-myc gene product. J Cell Biochem 73, 97–105.

Giorgio M, Trinei M, Migliaccio E, Pelicci PG (2007). Hydrogen peroxide: a metabolic by-product or a common mediator of ageing signals? Nat Rev Mol Cell Biol 8, 722–728.

Guy J, Hendrich B, Holmes M, Martin JE, Bird A (2001). A mouse Mecp2-null mutation causes neurological symptoms that mimic Rett syndrome. Nat Genet 27, 322–326.

Harborth J, Elbashir SM, Bechert K, Tuschl T, Weber K (2001). Identification of essential genes in cultured mammalian cells using small interfering RNAs. J Cell Sci 114, 4557–4565.

Harikrishnan KN *et al.* (2005). Brahma links the SWI/SNF chromatin-remodeling complex with MeCP2-dependent transcriptional silencing. Nat Genet 37, 254–264.

Helmbold H, Komm N, Deppert W, Bohn W (2009). Rb2/p130 is the dominating pocket protein in the p53-p21 DNA damage response pathway leading to senescence. Oncogene 28, 3456–3467.

Jones PL, Veenstra GJ, Wade PA, Vermaak D, Kass SU, Landsberger N, Strouboulis J, Wolffe AP (1998). Methylated DNA and MeCP2 recruit histone deacetylase to repress transcription. Nat Genet 19, 187–191.

Jori FP, Galderisi U, Piegari E, Peluso G, Cipollaro M, Cascino A, Giordano A, Melone MA (2001). RB2/p130 ectopic gene expression in neuroblastoma stem cells: evidence of cell-fate restriction and induction of differentiation. Biochem J 360, 569–577.

Jori FP, Melone MA, Napolitano MA, Cipollaro M, Cascino A, Giordano A, Galderisi U (2005a). RB and RB2/p130 genes demonstrate both specific and overlapping functions during the early steps of in vitro neural differentiation of marrow stromal stem cells. Cell Death Differ 12, 65–77.

Jori FP, Napolitano MA, Melone MA, Cipollaro M, Cascino A, Altucci L, Peluso G, Giordano A, Galderisi U (2005b). Molecular pathways involved in neural in vitro differentiation of marrow stromal stem cells. J Cell Biochem 94, 645–655.

Jori FP, Napolitano MA, Melone MA, Cipollaro M, Cascino A, Giordano A, Galderisi U (2004). Role of RB and RB2/P130 genes in marrow stromal stem cells plasticity. J Cell Physiol 200, 201–212.

Jung BP, Jugloff DG, Zhang G, Logan R, Brown S, Eubanks JH (2003). The expression of methyl CpG binding factor MeCP2 correlates with cellular differentiation in the developing rat brain and in cultured cells. J Neurobiol 55, 86–96.

Kapic A, Helmbold H, Reimer R, Klotzsche O, Deppert W, Bohn W (2006). Cooperation between p53 and p130(Rb2) in induction of cellular senescence. Cell Death Differ 13, 324–334.

Kim KY, Hysolli E, Park IY (2011). Neuronal maturation defect in induced pluripotent stem cells from patients with Rett syndrome. Proc Natl Acad Sci USA 108, 14169–14174.

Kimura H, Shiota K (2003). Methyl-CpG-binding protein, MeCP2, is a target molecule for maintenance DNA methyltransferase Dnmt1. J Biol Chem 278, 4806–4812.

Kishi N, Macklis JD (2004). MECP2 is progressively expressed in post-migratory neurons and is involved in neuronal maturation rather than cell fate decisions. Mol Cell Neurosci 27, 306–321.

Kishi N, Macklis JD (2010). MeCP2 functions largely cell-autonomously, but also non-cell-autonomously, in neuronal maturation and dendritic arborization of cortical pyramidal neurons. Exp Neurol 222, 51–58.

Luikenhuis S, Giacometti E, Beard CF, Jaenisch R (2004). Expression of MeCP2 in postmitotic neurons rescues Rett syndrome in mice. Proc Natl Acad Sci USA 101, 6033–6038.

Mullaney BC, Johnston MV, Blue ME (2004). Developmental expression of methyl-CpG binding protein 2 is dynamically regulated in the rodent brain. Neuroscience 123, 939–949.

Pittenger MF, Mackay AM, Beck SC, Jaiswal RK, Douglas R, Mosca JD, Moorman MA, Simonetti DW, Craig S, Marshak DR (1999). Multilineage potential of adult human mesenchymal stem cells. Science 284, 143–147.

Reynolds A, Leake D, Boese Q, Scaringe S, Marshall WS, Khvorova A (2004). Rational siRNA design for RNA interference. Nat Biotechnol 22, 326–330.

Ross RA, Spengler BA, Domenech C, Porubcin M, Rettig WJ, Biedler JL (1995). Human neuroblastoma I-type cells are malignant neural crest stem cells. Cell Growth Differ 6, 449–456.

Sambrook J, Russell D (2001). Molecular Cloning: A Laboratory Manual, Cold Spring Harbor, NY: Cold Spring Harbor Laboratory Press.

Shahbazian M, Young J, Yuva-Paylor L, Spencer C, Antalffy B, Noebels J, Armstrong D, Paylor R, Zoghbi H (2002). Mice with truncated MeCP2 recapitulate many Rett syndrome features and display hyperacetylation of histone H3. Neuron 35, 243–254.

Singh J, Saxena A, Christodoulou J, Ravine D (2008). MECP2 genomic structure and function: insights from ENCODE. Nucleic Acids Res 36, 6035–6047.

Squillaro T, Alessio N, Cipollaro M, Renieri A, Galderisi U (2008a). Silencing of methyl CpG binding protein 2 (MECP2) in mesenchymal stem cells induces senescence along with decreased expression of stemness-related genes. Presented at the 6th ISSCR Annual Meeting 2008, Philadelphia, PA, Poster Section, Abstract 80.

Squillaro T, Alessio N, Cipollaro M, Renieri A, Giordano A, Galderisi U (2010). Partial silencing of methyl cytosine protein binding 2 (MECP2) in mesenchymal stem cells induces senescence with an increase in damaged DNA. FASEB J 24, 1593–1603.

Squillaro T, Alessio N, Di Bernardo G, Cipollaro M, Renieri A, Giordano A, Galderisi U (2008b). Senescence of mesenchymal stem cells: the role of MeCP2 gene. Presented at What Is New in Europe in the Field of Regenerative Medicine? RESCUE Society Congress, 2008, Stockholm, Sweden.

Squillaro T, Hayek G, Farina E, Cipollaro M, Renieri A, Galderisi U (2008c). A case report: bone marrow mesenchymal stem cells from a Rett syndrome patient are prone to senescence and show a lower degree of apoptosis. J Cell Biochem 103, 1877–1885.

Stancheva I, Collins AL, Van den Veyver IB, Zoghbi H, Meehan RR (2003). A mutant form of MeCP2 protein associated with human Rett syndrome cannot be displaced from methylated DNA by notch in *Xenopus embryos*. Mol Cell 12, 425–435.

Tudor M, Akbarian S, Chen RZ, Jaenisch R (2002). Transcriptional profiling of a mouse model for Rett syndrome reveals subtle transcriptional changes in the brain. Proc Natl Acad Sci USA 99, 15536–15541.

Weaving LS, Ellaway CJ, Gecz J, Christodoulou J (2005). Rett syndrome: clinical review and genetic update. J Med Genet 42, 1–7.

Woodbury D, Schwarz EJ, Prockop DJ, Black IB (2000). Adult rat and human bone marrow stromal cells differentiate into neurons. J Neurosci Res 61, 364–370.

Yasui DH, Peddada S, Bieda MC, Vallero RO, Hogart A, Nagarajan RP, Thatcher KN, Farnham PJ, Lasalle JM (2007). Integrated epigenomic analyses of neuronal MeCP2 reveal a role for long-range interaction with active genes. Proc Natl Acad Sci USA 104, 19416–19421.